

On the parameter estimation for diffusion models of single neuron's activities

I. Application to spontaneous activities of mesencephalic reticular formation cells in sleep and waking states

Junko Inoue, Shunsuke Sato, Luigi M. Ricciardi*

Department of Biophysical Engineering, Faculty of Engineering Science, Osaka University, Toyonaka, Osaka 560, Japan

Received: 10 October 1994/Accepted in revised form: 21 March 1995

Abstract. For the Ornstein-Uhlenbeck neuronal model a quantitative method is proposed for the estimation of the two parameters characterizing the unknown input process, namely the neuron's mean input per unit time μ and the infinitesimal standard deviation per unit time σ . This method is based on the experimentally observed first- and second-order moments of interspike intervals. The dependence of the estimates $\hat{\mu}$ and $\hat{\sigma}$ on the moments of the observed interspike intervals and on the neuronal parameters is clarified, and a comparison is made between the estimates based on the classical Wiener model and those yielded by the Ornstein-Uhlenbeck model. Comprehensive tables are included in which the displayed values of $\hat{\mu}$ and $\hat{\sigma}$ have been calculated in terms of physiologically realistic pairs of first- and second-order moments. Our method is finally applied to interspike interval data recorded from neurons in the mesencephalic reticular formation of the cat during hypothetical sleep, slow-wave sleep stage, and wake stage.

1 Introduction

One-dimensional diffusion processes have been widely used as models to account for statistical features of spike trains recorded from single neurons belonging to complex networks in the brain. Among these, the Ornstein-Uhlenbeck (OU) process plays a central role because it naturally arises when starting from an equivalent electric circuit of the membrane potential of real neurons at subthreshold level. The corresponding neuronal model is thus referred to as the OU model.

In general, diffusion models of neuronal activity arise when it is assumed, or proved, that the membrane potential

is described by a stochastic process $X(t)$ that satisfies the stochastic differential equation

$$dX(t) = \mu(X(t))dt + \sigma(X(t))dW(t), \quad P\{X(0) = x_0\} = 1 \quad (1)$$

where $W(t)$ is the standard Wiener process, $\mu(\cdot)$ and $\sigma(\cdot)$ are functions of $X(t)$ accounting for neuronal input processes, and x_0 denotes the initial potential.

We assume that neuronal firing takes place, and consequently an action potential (spike) is observed, whenever the neuron's membrane potential $X(t)$ reaches the firing threshold $S(t)$ and that the membrane potential is then instantly reset to the initial membrane potential x_0 . The threshold potential $S(t)$ is commonly taken to be a deterministic time function. However, we shall assume throughout this paper that it is constant, i.e., $S(t) = S$. The interspike interval (ISI) is then represented by the random variable

$$T_S = \inf\{t \geq 0: X(t) \geq S\}, \quad X(0) = x_0 < S \quad (2)$$

namely, by the first-passage time (FPT) through S of the process $X(t)$ conditional on the initial value x_0 . Although we call $X(t)$, x_0 , and S the membrane potential, the initial potential, and the threshold, respectively, we assume in the sequel that these symbols imply the differences between respective potentials and the membrane resting potential, for the sake of convenience. The FPT probability density function (pdf)

$$g(t|S, x_0) = \frac{\partial}{\partial t} P\{T_S \leq t\}, \quad 0 \leq t < \infty$$

is thus appropriate to describe the time interval elapsing between successive spikes. In other words, it is assumed that the ISIs are generated in accordance with a renewal process associated to the FPTs (T_S). Therefore, all theoretical studies on diffusion neuronal models are ultimately focused on the FPT problem for the underlying process. Despite the conceptual simplicity of most diffusion models, it is hard to solve the corresponding FPT problems as

*Permanent address: Dipartimento di Matematica e Applicazioni, Università di Napoli "Federico II", Via Cintia, I-80126 Napoli, Italy
Correspondence to: Dr. Junko Inoue

in general they are analytically intractable and numerically difficult to handle.

The first diffusion model for neuronal activity was suggested by Gerstein and Mandelbrot (1964). In this model – also known as the Wiener or perfect integrator neuronal model – the membrane potential $X(t)$ is described by a Wiener process with positive drift, i.e., by the diffusion process defined by (1) with

$$\mu(\cdot) = \mu > 0, \quad \sigma(\cdot) = \sigma > 0 \quad (3)$$

The parameters μ and σ denote, respectively, the mean input per unit time to the neuron and the positive square root of the variance per unit time (drift and infinitesimal standard deviation). The FPT pdf for this model, which is the theoretical counterpart of the ISI histogram, is the well-known inverse gaussian distribution (IGD). However, it should be stressed that this is a model too simple to be realistically viewed as suitable to describe the neuron's membrane potential in general.

In the OU model, also known as the leaky integrator, the underlying diffusion process $X(t)$ is specified by

$$\mu(x) = -\frac{x}{\tau} + \mu, \quad \sigma(x) = \sigma > 0 \quad (4)$$

where μ is the mean input per unit time to the neuron, σ^2 the variance per unit time, and τ the membrane time constant ($-\infty < \mu < \infty$, $\sigma < 0$, $\tau > 0$). For any value of μ , the first-passage through S is a sure event ($P\{T_S < \infty\} = 1$). This model, that realistically includes the spontaneous decay of the membrane potential to the resting value, is generally accepted as the simplest and most reasonable compromise for modeling the spontaneous activity of neurons in the central nervous system, and it is also used as a basis for the most common stochastic models of single neurons (Ricciardi 1976, 1977; Tuckwell 1988, 1989; Lánský et al. 1990; Rospars and Lánský 1993).

The OU process, which is also appropriate to describe a variety of fluctuating phenomena besides neuronal discharges, has been widely analyzed. In particular, an expression for the Laplace transform of the FPT pdf has been obtained (Roy and Smith 1969), and by using a singular point analysis of the Laplace transform, the FPT pdf has been expressed as an infinite sum of exponential functions with negative exponents (Ricciardi and Sato 1988). Numerical methods for the evaluation of the FPT pdf have also been proposed (Buonocore et al. 1987), since manageable analytical results are scarce and fragmentary. Because of the unavailability of closed-form results for the FPT pdf, a considerable amount of work has been directed to the study of the FPT moments. Explicit moment formulas have been given (Keilson and Ross 1975; Nobile et al. 1985; Ricciardi and Sato 1988), while the asymptotic behavior of the pdf as well as of moments has been studied (Tuckwell 1982; Nobile et al. 1985; Ricciardi and Sato 1988; Giorno et al. 1990). The formulas for the moments, however, are rather cumbersome, so that numerical evaluations constitute a formidable task.

More realistic models, such as those that take into account the reversal potentials (Capocelli and Ricciardi 1973; Hanson and Tuckwell 1983; Smith and Smith 1984; Lánský and Lánská 1987; Giorno et al. 1988), have also been proposed, but it is usually impossible to obtain their FPT pdf's. In the rare cases where this can be done, the FPT pdf is in the form of a rather complicated function whose behavior is hard to discern. This is the reason why models more realistic than the Wiener one, such as the OU model, have not been analyzed so far with reference to real experimental data (Tuckwell and Richter 1978). In particular, the problem of the parameters estimation for the OU model has not been considered on a rigorous quantitative basis.

As for the experimental evidence, we recall that the spontaneous firings of single neurons in the central nervous system have been often systematically recorded and analyzed (see, for instance, Correia and Landolt 1977; Anastasio et al. 1985; Lánský and Radil 1987; Levine 1991; see also the references in Tuckwell 1988). Stationarity and independence of neuronal spike series have been discussed, and the frequency distribution of the observed ISIs has been fitted by means of theoretical distributions such as gamma, IGD, and log-normal, and the goodness of fit has been discussed.

According to the above investigations, the fitness of the data of IGD or log-normal distribution is good. However, this is a purely phenomenological approach in which values of physicochemical variables relevant to the real neuronal firings, such as the intensity or the variance of synaptic input, cannot be estimated because such distributions do not arise as a consequence of the consideration of any physicochemical process underlying spike generation. Instead, methods to estimate the values of parameters such as $\mu(\cdot)$ and $\sigma(\cdot)$ have been proposed by observing not the extracellularly recorded spike sequences but the intracellularly recorded subliminal membrane potential fluctuation (Lánský 1983; Lánský et al. 1988; Habib 1992).

In the present paper, we assume that the neuronal firing is modeled by the OU process and propose a method to obtain quantitative evaluations of the input parameters μ and σ from the first and second sample moments of ISI based on the OU model in which physiologically plausible values of the 'intrinsic' parameters x_0 , S and τ are preassigned. The dependence of estimates $\hat{\mu}$ and $\hat{\sigma}$ on the assumed values of parameters x_0 , S , and τ is then clarified on the basis of extensive and systematic numerical computation results.

The relation between the moments of the observed ISIs and the estimates $\hat{\mu}$ and $\hat{\sigma}$ is established by using the mean ISI and its coefficient of variation (CV = standard deviation/mean). It should be stressed that the CV is widely used by both theoretical and experimental neurobiologists as it is appropriate to quantify the degree of regularity, or of randomness, of a spike train. A table will be given in which the values of $\hat{\mu}$ and $\hat{\sigma}$ have been estimated by means of physiologically plausible pairs of the first- and second-order moments. A comparison based on the Wiener model and on the OU model will finally be performed between the values of parameters

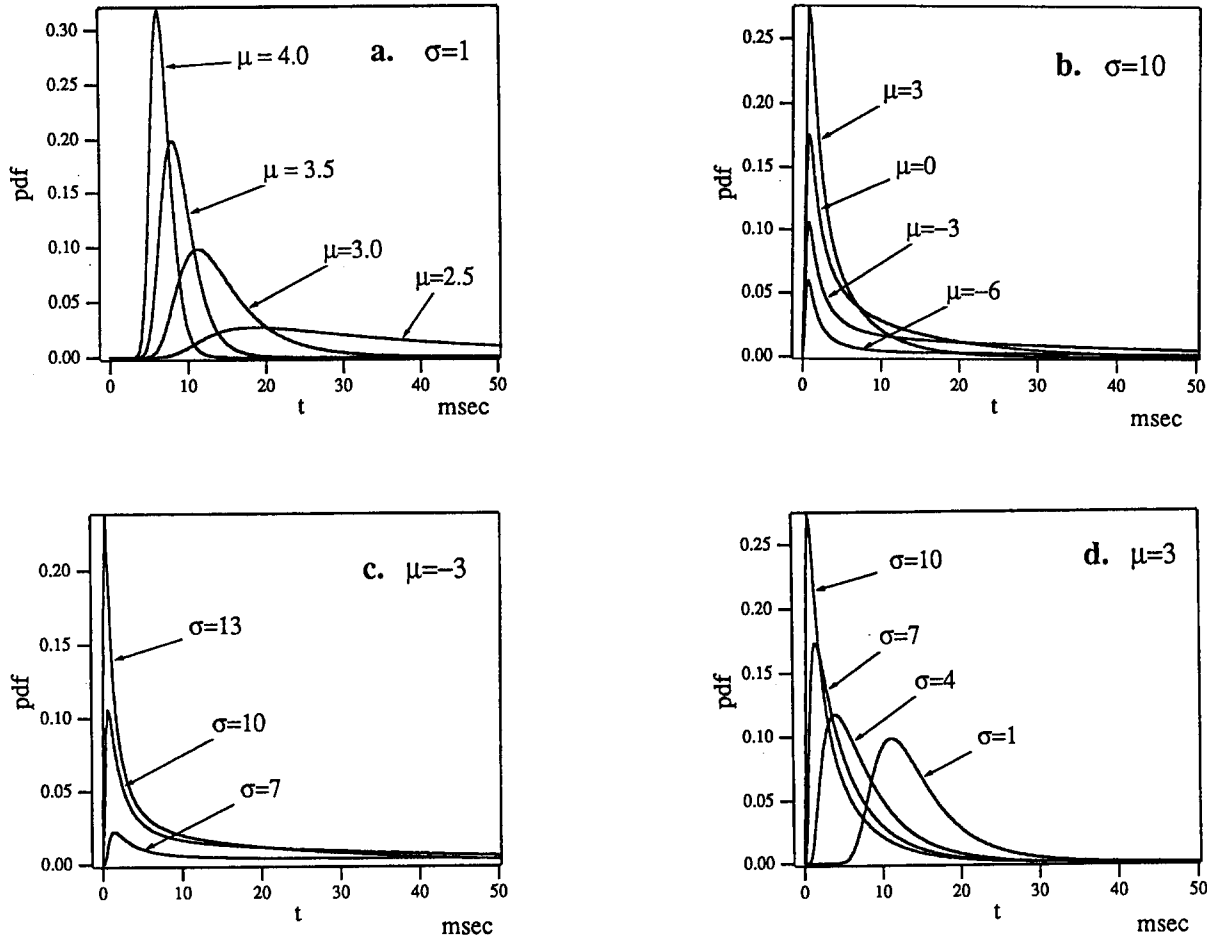


Fig. 1. Ornstein-Uhlenbeck first-passage time probability density functions (OU-FPT pdf's) for various pairs of μ and σ . All pdf's are obtained by setting $x_0 = 0$, $S = 15$, and $\tau = 5$. In (a) $\sigma = 1$ and $\mu = 2.5, 3.0, 3.5,$

4.0; in (b) $\sigma = 10$ and $\mu = -6, -3, 0, 3$; in (c) $\mu = -3$ and $\sigma = 7, 10, 13$; and in (d) $\mu = 3$ and $\sigma = 1, 4, 7, 10$

estimated for the ISIs observed from neurons in mesencephalic reticular formation of cat during hypothetical sleep, slow-wave sleep stage, and wake stage.

2 The FPT problem for the OU neuronal model

2.1 Normalization of the OU process

As we have seen in Sect. 1, the FPT pdf of the OU process to a constant boundary, which is the theoretical counterpart of the ISI histogram, depends on the five parameters μ , σ , S , x_0 , and τ , where μ and σ are related to the neuronal input, whereas S , x_0 , and τ are intrinsic or characteristic parameters of the neuron. The FPT pdf's for various pairs of input parameters are plotted in Fig. 1, where we have set $x_0 = 0$, $S = 15$, and $\tau = 5$. They have been obtained numerically by means of the algorithm proposed in Buonocore et al. (1987).

To reduce the number of parameters in (1) with (4), we make use of the transformation

$$x' = \sqrt{2/\sigma^2\tau}(x - \mu\tau), \quad t' = \frac{t}{\tau} \quad (5)$$

The process $X(t)$ defined as a solution of (1) with (4) is then transformed into the process $X'(t')$ which satisfies $dX'(t') = -X'(t')dt' + \sqrt{2}dW(t')$, $P\{X'(0) = \xi\} = 1$ (6)

with new initial state ξ and new threshold η given by

$$\xi = \sqrt{2/\sigma^2\tau}(x_0 - \mu\tau) \quad (7a)$$

$$\eta = \sqrt{2/\sigma^2\tau}(S - \mu\tau), \quad -\infty < \xi < \eta < \infty \quad (7b)$$

We shall refer to $X'(t')$ as the 'normalized' OU process. It is not difficult to prove that the following relations hold:

$$g(S, t | x_0) = g'(\eta, t' | \xi) \left| \frac{dt'}{dt} \right| = \frac{1}{\tau} g'(\eta, t/\tau | \xi) \quad (8a)$$

$$m_n(S | x_0) = \tau^n M_n(\eta | \xi) \quad (8b)$$

where $g(S, t | x_0)$ is the FPT pdf of $X(t)$, $g'(\eta, t' | \xi)$ is that of $X'(t')$, and where for $n = 1, 2, \dots$

$$m_n(S | x_0) = \int_0^{\infty} t'^n g(S, t | x_0) dt, \quad M_n(\eta | \xi) = \int_0^{\infty} (t')^n g'(\eta, t' | \xi) dt'$$

denote the moment of order n of the FPT of $X(t)$ and of $X'(t)$, respectively. Note that $X(t)$ and $X'(t')$ possess identical coefficients of variation. Hence, in the sequel such a coefficient of variation will be denoted for both processes by the unique symbol CV.

The FPT of the normalized OU process to a constant boundary η is a random variable depending on the two parameters (ξ, η) , and hence via (8), the FPT of the OU process to a constant boundary S is a random variable depending on the triplet of parameters (ξ, η, τ) .

2.2 FPT moments

There exist several alternative formulas and analytical approximate results for the moments $M_n(\eta|\xi)$ of the normalized OU process (Keilson and Ross 1975; Tuckwell 1982; Nobile et al. 1985; Ricciardi and Sato 1988). They are all very cumbersome and thus hard to use for reliable numerical computations.

Let us employ the following explicit expressions by Ricciardi and Sato (1988) for the first two moments:

$$M_1(\eta|\xi) = \phi_1(\eta) - \phi_1(\xi) \quad (9a)$$

$$M_2(\eta|\xi) = 2\phi_1^2(\eta) - \phi_2(\eta) - 2\phi_1(\eta)\phi_1(\xi) + \phi_2(\xi) \quad (9b)$$

where we have taken $\eta \geq \xi$. In (9), the expressions for $\phi_k(z)$, $k = 1, 2$ are given by:

$$\phi_k(z) = \frac{k}{2^k} \sum_{n=1}^{\infty} \frac{(\sqrt{2z})^n}{n!} \Gamma\left(\frac{n}{2}\right) \rho_n^{(k)}, \quad (k = 1, 2, \dots) \quad (10a)$$

$$\rho_n^{(1)} = 1, \quad \rho_n^{(2)} = \psi(n/2) - \psi(1) \quad (10b)$$

where $\Gamma(\gamma)$ and $\psi(\gamma)$ denote the gamma function and the digamma function, respectively. Expressions (10) are useful for numerical calculation of $\phi_k(z)$ whenever $z \geq 0$ and $|z|$ is rather small. If, instead, $z < 0$ and $|z|$ is large, alternative expressions must be used, as we shall see in the sequel. Indeed, for $z < 0$, the evaluation of $\phi_k(z)$, which is an alternating series [see (10)], becomes harder and harder as the value of $|z|$ grows larger, because of canceling effects. Hence, a different method is needed to estimate $\phi_k(z)$ when z is negative and rather large in absolute value. Good approximations of $\phi_k(z)$ can be obtained in such cases, by making use of the following results due to Keilson and Ross (1975):

$$\phi_1(z) \simeq - \left(K_B + \log|z| + \sum_{k=1}^{\infty} \frac{b_k}{z^{2k}} \right) \quad (11a)$$

$$\phi_2(z) \simeq 2 \left[K_D + K_B \log|z| + \frac{1}{2} (\log|z|)^2 + \sum_{k=1}^{\infty} b_k \frac{\log|z|}{z^{2k}} + \sum_{k=1}^{\infty} \frac{g_k}{z^{2k}} \right], \quad (11b)$$

where $K_B = 0.63518142$, $K_D = 0.818578$ and

$$a_k = \frac{(-1)^{k-1} (2k-2)!}{(k-1)! 2^{k-1}} \quad b_k = -\frac{a_{k+1}}{2k}$$

$$c_k = a_k + b_k \quad d_k = c_k - (2k-1)d_{k-1}$$

$$g_k = K_B b_k - \frac{a_{k+1}}{4k^2} - \frac{d_k}{2k}$$

Expressions (10) and (11) have been used to evaluate $\phi_k(z)$ at $z = -7$, and results from both expressions are in excellent agreement.

3 Parameter estimation from first and second FPT moments

3.1 Method of moments

Suppose that first and second sample moments (m_1, m_2) of ISI are obtained from an experiment. Because the theoretical counterpart of the ISI is the FPT in the OU model, we can equate sample and FPT moments:

$$\tau M_1(\eta|\xi) = m_1 \quad (12a)$$

$$\tau^2 M_2(\eta|\xi) = m_2 \quad (12b)$$

or, alternatively to (12b),

$$\frac{\sqrt{M_2(\eta|\xi) - M_1^2(\eta|\xi)}}{M_1(\eta|\xi)} = \text{CV} \quad (12c)$$

Let us now assign a reasonable value to τ , which is legitimate since τ is one of the intrinsic neuronal parameters. Making use of analytical and/or approximate expressions (9) for the moments $M_1(\eta|\xi)$ and $M_2(\eta|\xi)$, we can then obtain estimates $\hat{\xi}$ and $\hat{\eta}$ by numerically solving (12). Finally, by virtue of (7), we are led to the estimates $\hat{\mu}$ and $\hat{\sigma}$ of the input parameters from the estimates $\hat{\xi}$ and $\hat{\eta}$:

$$\hat{\mu} = \frac{1}{\bar{\tau}} \frac{\hat{\eta} \bar{x}_0 - \hat{\xi} \bar{S}}{\hat{\eta} - \hat{\xi}} \quad \hat{\sigma} = \sqrt{\frac{2}{\bar{\tau}} \frac{\bar{S} - \bar{x}_0}{\hat{\eta} - \hat{\xi}}} \quad (13)$$

where \bar{x}_0 , \bar{S} , and $\bar{\tau}$ denote the assumed values of intrinsic neuronal parameters x_0 , S , τ . The difference S between threshold and resting potential can be assumed to be of the order of 10–20 mV and the time constant τ to range from 1 to 20 ms in different neurons (see, for example, Kandel and Schwartz 1985). The difference x_0 between the initial membrane potential and the resting potential will be taken as zero in the simplest case.

The FPT pdf $g'(\hat{\eta}, t/\bar{\tau}|\hat{\eta})$ can then be obtained by a numerical method (see, for instance, Buonocore et al. 1987), and hence via (8a) one can obtain the FPT pdf $g(\bar{S}, t|\bar{x}_0)$ which corresponds to the ISI histogram of the neuronal model with assumed \bar{S} , \bar{x}_0 , and $\bar{\tau}$ as the values of its intrinsic parameters and with $\hat{\mu}$ and $\hat{\sigma}$ as the estimates of input parameters.

When one solves (12), due to the circumstance that $M_1(\eta|\xi)$ and $M_2(\eta|\xi)$ have been obtained as sums of power series in ξ and η , their derivatives with respect to ξ and η can be calculated. Equations (12) can then be solved with respect to ξ and η by standard methods, such as Newton's method. [Approximate expressions for $d\phi_k(z)/dz$ when z is negative and large in absolute value can also be obtained by formally differentiating the right-hand side of (11) with respect to z .] However, it must be pointed out that for an effective implementation of Newton's method, an appropriate choice of the initial value is required. To overcome the difficulty inherent in the

Table 1. Estimated parameters ξ and $\hat{\eta}$ obtained from the FPT moments via (12). The FPT moments have been computed by means of the moment formulas (9) via (8b) for choices (τ^*, ξ^*, η^*) . The computed FPT moments $m_1 = \tau^* M_1(\eta^* | \xi^*)$ and $m_2 = \tau^{*2} M_2(\eta^* | \xi^*)$ were obtained numerically in two ways, i.e. by an accuracy to five decimal digits ($m_1^{(5)}$ and $m_2^{(5)}$) and two decimal digits ($m_1^{(2)}$ and $m_2^{(2)}$). The estimates $\xi^{(5)}$ and $\hat{\eta}^{(5)}$ are obtained from $m_1^{(5)}$ and $m_2^{(5)}$ and $\xi^{(2)}$ and $\hat{\eta}^{(2)}$ from $m_1^{(2)}$ and $m_2^{(2)}$

ξ^*	η^*	$m_1^{(5)}$	$m_2^{(5)}$	$\xi^{(5)}$	$\hat{\eta}^{(5)}$	$m_1^{(2)}$	$m_2^{(2)}$	$\xi^{(2)}$	$\hat{\eta}^{(2)}$
1	3	84.838	14616	1.0000	3.0000	85	15000	1.4	3.0
-3	-1	0.88044	1.0684	-3.0001	-1.0001	0.88	1.1	-2.8	-0.89

choice of the initial point, Newton's method and a continuation method (see, for instance, Ortega and Rheinboldt 1970) have been combined.

In order to check the validity and effectiveness of our numerical computation mentioned above, we have applied it to some test cases. The values τ^* , ξ^* , and η^* of parameters τ , ξ , and η have been preassigned, and the FPT moments $\tau^* M_1(\eta^* | \xi^*)$ and $\tau^{*2} M_2(\eta^* | \xi^*)$ have been computed numerically with different accuracies for such choices by means of (8b) and (9). By $m_1^{(5)}$ and $m_2^{(5)}$, we indicate an accuracy to five significant digits by $m_1^{(2)}$ and $m_2^{(2)}$ an accuracy to two significant digits. The results are shown in Table 1. It is evident that the estimates $\xi^{(5)}$ and $\hat{\eta}^{(5)}$ are characterized by an excellent precision. It is also clear that estimates $\xi^{(2)}$ and $\hat{\eta}^{(2)}$ do not differ too drastically from estimates $\xi^{(5)}$ and $\hat{\eta}^{(5)}$ of $m_1^{(5)}$ and $m_2^{(5)}$. This indicates that our method is not very sensitive to the measurement error of the sample moments m_1 and m_2 and that it is stable.

3.2 Dependence of estimates on FPT moments

Let us consider the quantities $\hat{\mu}\bar{\tau} = \hat{\mu}\bar{\tau}(M_1, CV)$ and $\hat{\sigma}\sqrt{\bar{\tau}} = \hat{\sigma}\sqrt{\bar{\tau}}(M_1, CV)$ as compound functions of the normalized mean $M_1 (\equiv m_1/\tau)$ and of the coefficient of variation (CV) $\equiv CV$ of the FPT. From (13), we have

$$\hat{\mu}\bar{\tau} = \frac{\hat{\eta}\bar{x}_0 - \xi\bar{S}}{\hat{\eta} - \xi}, \quad \hat{\sigma}\sqrt{\bar{\tau}} = \sqrt{2} \frac{\bar{S} - \bar{x}_0}{\hat{\eta} - \xi} \quad (14)$$

Note that the estimated mean input $\hat{\mu}\bar{\tau}$ and its variance $\hat{\sigma}^2\bar{\tau}$ per time duration $\bar{\tau}$ depend only on the two quantities M_1 and CV. Using this remark, we shall provide numerical tables (cf. Tables 3 and 4) in which $\hat{\mu}\bar{\tau}$ and $\hat{\sigma}\sqrt{\bar{\tau}}$ are displayed for a variety of values of M_1 and CV. For any fixed $\bar{\tau}$ the desired estimates of $\hat{\mu}$ and $\hat{\sigma}$ will then follow. Although we have set $\bar{S} = 15$ and $\bar{x}_0 = 0$ as a realistic possibility to obtain Tables 3 and 4, the effect of different choices of \bar{S} and \bar{x}_0 on the estimates $\hat{\mu}$ and $\hat{\sigma}$ will be considered in the following section.

Figures 2 and 3 show the dependence of the estimated input mean $\hat{\mu}\bar{\tau}$ and the standard deviation $\hat{\sigma}\sqrt{\bar{\tau}}$ on the normalized FPT mean M_1 and CV for the choice $(\bar{x}_0, \bar{S}) = (15, 0)$. As shown in Fig. 2a, when $CV \geq 1$, $\hat{\mu}\bar{\tau}$ decreases as M_1 increases and is negative except for small values of M_1 . The sign of $\hat{\mu}\bar{\tau}$ changes around $M_1 = 6.5$ when $CV = 1$, and the value of M_1 where a change of sign takes place becomes smaller as the CV grows larger, as shown in Fig. 2a. When $CV < 1$, $\hat{\mu}\bar{\tau}$ decreases as M_1

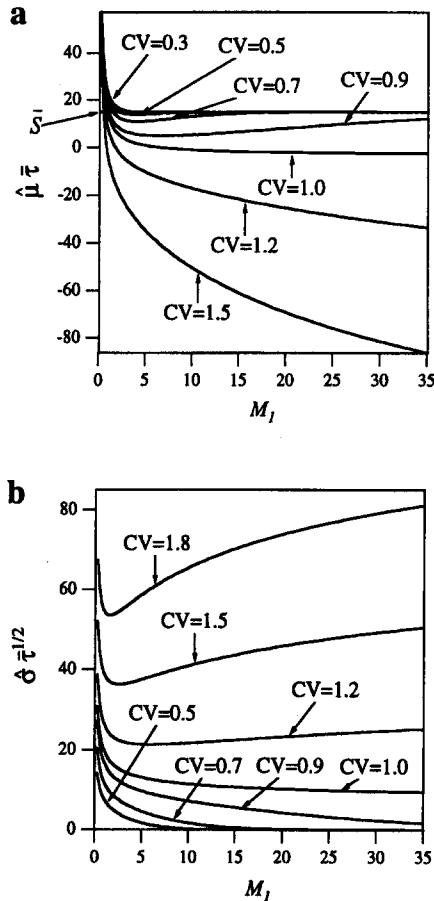


Fig. 2a, b. Dependence on the normalized FPT mean M_1 of the estimated input parameters for various fixed values of the coefficient of variation (CV), with $\bar{x}_0 = 0$ and $\bar{S} = 15$. (a) Dependence on M_1 of the estimated mean input $\hat{\mu}\bar{\tau}$ per time duration $\bar{\tau}$; (b) dependence on M_1 of the square root of the estimated input variance $\hat{\sigma}^2\bar{\tau}$ per time duration $\bar{\tau}$

increases to reach its minimum and then increases to approach asymptotically the threshold value ($\bar{S} = 15$). Figure 4a shows the minimum of $\hat{\mu}\bar{\tau}$, $(\hat{\mu}\bar{\tau})_{\min}$, for various choices of $CV < 1$. Note that $\hat{\mu}\bar{\tau}$ is almost always positive when $CV < 1$. From the plots of the results of our computations it is evident that an increase of the FPT mean does not necessarily imply a decrease of the input mean $\hat{\mu}\bar{\tau}$: A result that is as interesting as unexpected and that appears to have passed so far unnoticed.

As for the quantity $\hat{\sigma}\sqrt{\bar{\tau}}$, this has a minimum for each $CV > 1$ (see Fig. 2b). Such a minimum, $(\hat{\sigma}\sqrt{\bar{\tau}})_{\min}$, has been indicated in Fig. 4b. In contrast to the behavior of

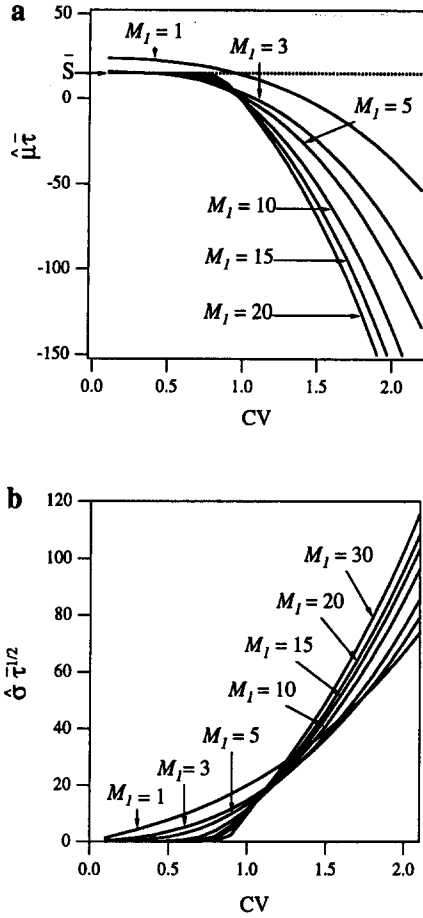


Fig. 3a, b. Dependence on CV of the estimated input parameters of the FPT for various fixed values of M_1 and for $\bar{x}_0 = 0$ and $\bar{S} = 15$. In (a) the dependence on CV of the estimated mean input $\hat{\mu}\bar{\tau}$ per time duration $\bar{\tau}$ is shown, whereas in (b) the dependence on CV of the square root of the estimated input variance $\hat{\sigma}^2\bar{\tau}$ per time duration $\bar{\tau}$ is indicated

$(\hat{\mu}\bar{\tau})_{\min}$, the relation between CV and $(\hat{\sigma}\sqrt{\bar{\tau}})_{\min}$ appears to be almost linear. The estimate $\hat{\sigma}\sqrt{\bar{\tau}}$ strongly depends on the CV, and the diversity of the means seems to be rather ineffective (cf. Fig. 3b). If $(\hat{\sigma}\sqrt{\bar{\tau}})_{\min}$ is estimated via CV, then a rough approximation of $\hat{\sigma}\sqrt{\bar{\tau}}$ also follows. Indeed, as Fig. 2b shows, for each fixed CV the corresponding quantity $\hat{\sigma}\sqrt{\bar{\tau}}$ does not vary rapidly with M_1 . Moreover, the estimated quantities $\hat{\sigma}\sqrt{\bar{\tau}}$ remain clearly distinct as CV is varied.

It is meaningful to remark that, as Fig. 2a and Fig. 3a indicate, for most of the region of variability of M_1 and CV the ensuing estimated quantity $\hat{\mu}\bar{\tau}$ is below the firing threshold ($\bar{S} = 15$ in figures). Under such conditions no output would be released by the model neuron in the absence of randomness [namely, if $\sigma \rightarrow 0$ in (4)], i.e., in the limit of a deterministic model. The presence of randomness thus ensures the existence of a firing activity by the model neuron (see Fig. 2b).

3.3 Dependence of estimates on intrinsic parameters

For the estimation of the input parameters μ and σ , values for the intrinsic parameters S , x_0 , and τ must be

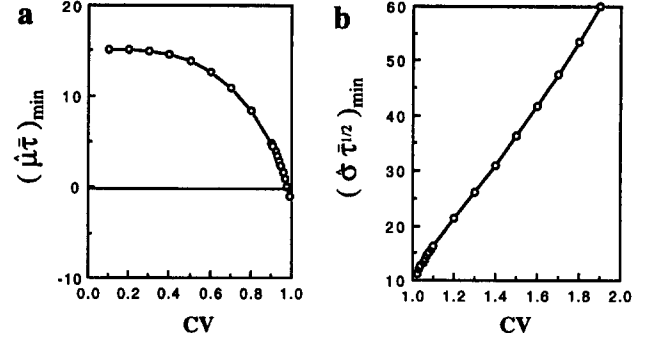


Fig. 4a, b. The minimum of the estimated input parameters for various choices of CV. (a) The minimum of $\hat{\mu}\bar{\tau}$ for various choices of CV < 1; (b) the minimum of $\hat{\sigma}\sqrt{\bar{\tau}}$ for various choices of CV > 1

assumed. As is well known, the values of S and τ in general depend both on the type of neuron and on its state. Although the initial state x_0 is often set to zero, we can set it to any value. For instance, by setting $x_0 = -10$ mV the effect of afterhyperpolarization can be taken into account. We shall now discuss the dependence of $\hat{\mu}$ and $\hat{\sigma}$ on the values of \bar{x}_0 , \bar{S} , and $\bar{\tau}$.

First of all, consider the effect of the assumed values \bar{x}_0 and \bar{S} on the estimates $\hat{\mu}$ and $\hat{\sigma}$. Suppose now that $\hat{\mu}_1$ and $\hat{\sigma}_1$ are the estimates obtained from the choices $\bar{\tau}$, $\bar{x}_0 = \bar{x}_{01}$ and $\bar{S} = \bar{S}_1$, and $\hat{\mu}_2$ and $\hat{\sigma}_2$ are those from $\bar{\tau}$, $\bar{x}_0 = \bar{x}_{02}$, and $\bar{S} = \bar{S}_2$. From (13), we obtain the relation between $\hat{\mu}_1$ and $\hat{\mu}_2$ and that between $\hat{\sigma}_1$ and $\hat{\sigma}_2$:

$$\frac{\hat{\mu}_1}{\hat{\mu}_2} = \frac{\hat{\eta}\bar{x}_{01} - \hat{\xi}\bar{S}_1}{\hat{\eta}\bar{x}_{02} - \hat{\xi}\bar{S}_2}, \quad \frac{\hat{\sigma}_1}{\hat{\sigma}_2} = \frac{\bar{S}_1 - \bar{x}_{01}}{\bar{S}_2 - \bar{x}_{02}} \quad (15)$$

In the particular case $\bar{x}_{01} = \bar{x}_{02} = 0$, from (15), we have the simple linear relations

$$\frac{\hat{\mu}_1}{\hat{\mu}_2} = \frac{\bar{S}_1}{\bar{S}_2}, \quad \frac{\hat{\sigma}_1}{\hat{\sigma}_2} = \frac{\bar{S}_1}{\bar{S}_2} \quad (16)$$

The dependence of the estimated input parameters on the time constant $\bar{\tau}$ is more complicated. Figure 5 shows the changes of the estimated input parameters $\hat{\mu}$ and $\hat{\sigma}$ as a function of $\bar{\tau}$ for fixed values of the FPT moments ($m_1 = 20$, CV = 0.5, 0.8, 1.0, 2.0), where we have set $\bar{x}_0 = 0$ and $\bar{S} = 15$. We recall that the OU process yields the Wiener process in the limit when the time constant τ tends to infinity [see (3) and (4)]. In Fig. 5, $\hat{\mu}_w$ and $\hat{\sigma}_w$ denote the mean input per unit time to the neuron and the standard deviation per unit time for the Wiener model estimated from the same values of moments via the closed form expressions

$$\hat{\mu}_w = \frac{\bar{S} - \bar{x}_0}{m_1} \quad (17)$$

$$\hat{\sigma}_w = (\bar{S} - \bar{x}_0) \sqrt{\frac{m_2 - m_1^2}{m_1^3}} = (\bar{S} - \bar{x}_0) \frac{\text{CV}}{\sqrt{m_1}} \quad (18)$$

Parameter $\hat{\mu}_w$ is proportional to the firing rate (m_1^{-1}) and is always positive. The estimated standard deviation $\hat{\sigma}_w$ of the input per unit time is proportional to CV for fixed m_1 and decreases as m_1 increases.

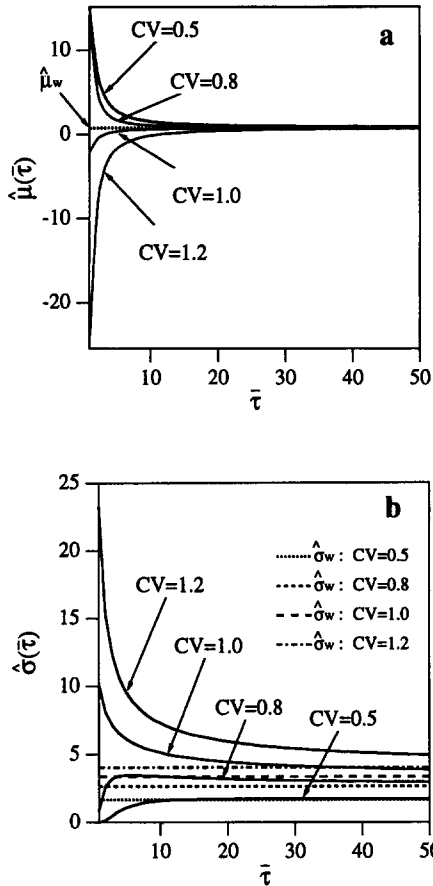


Fig. 5a, b. Dependence of the estimated input parameters on the pre-assigned time constant $\bar{\tau}$ for fixed values of the FPT moments, where we have set $m_1 = 20$ and $CV = 0.5, 0.8, 1.0,$ and 1.2 , respectively, and with the choices $\bar{x}_0 = 0$ and $S = 15$. (a) Dependence of $\hat{\mu}$ on $\bar{\tau}$, where $\hat{\mu}_w$ denotes the estimated drift for the Wiener model; (b) dependence of $\hat{\sigma}$ on $\bar{\tau}$, where $\hat{\sigma}_w^2$ denotes the estimated infinitesimal variance for the Wiener model

The estimated parameters for the OU model depend nonlinearly on the assumed value $\bar{\tau}$. Indeed, the estimates $\hat{\mu} = \hat{\mu}(\bar{\tau})$ and $\hat{\sigma} = \hat{\sigma}(\bar{\tau})$ change largely with $\bar{\tau}$ for small values of $\bar{\tau}$ with modalities that vary according to the values of CV . Indeed, as shown in Fig. 5, $\hat{\mu}(\bar{\tau})$ decreases monotonically when $CV < 1$ and increases when $CV \geq 1$ to approach $\hat{\mu}_w$ in both cases. In particular, we note that the sign of $\hat{\mu}(\bar{\tau})$ depends on the assumed value of τ when $CV \geq 1$. Since the sign of $\hat{\mu}(\bar{\tau})$ indicates whether excitatory inputs prevail over inhibitory inputs, or vice versa, an observed change of the sign of $\hat{\mu}(\bar{\tau})$ when the assumed value $\bar{\tau}$ is changed does indicate a qualitatively significant different result for the estimated parameter. As for the estimate $\hat{\sigma}$, Fig. 5b shows that for $CV \geq 1$, $\hat{\sigma}(\bar{\tau})$ decreases to approach $\hat{\sigma}_w$ asymptotically, whereas if $CV < 1$, $\hat{\sigma}(\bar{\tau})$ initially increases and then decreases to approach $\hat{\sigma}_w$ asymptotically. Note that the speed of convergence to $\hat{\sigma}_w$ decreases as CV increases. Hence, the assumed value of τ used in the estimation considerably affects the resulting estimated values of parameters.

Figure 6 depicts the dependence of the estimated FPT pdf on $\bar{\tau}$ for the OU model. Figure 6a shows the case when $m_1 = 20$ and $CV = 0.5$, Fig. 6b refers to the case in

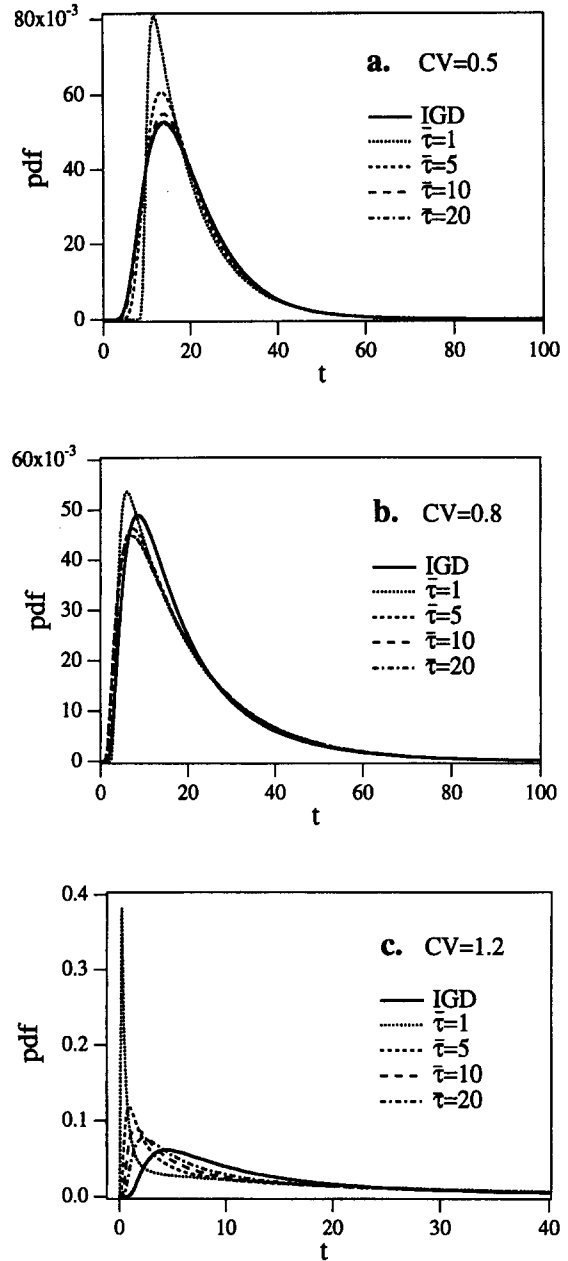


Fig. 6a-c. Dependence of the estimated FPT pdf on $\bar{\tau}$ for the OU model: (a) $m_1 = 20$ and $CV = 0.5$; (b) $m_1 = 20$ and $CV = 0.8$; (c) $m_1 = 20$ and $CV = 1.2$

which $m_1 = 20$ and $CV = 0.8$, while Fig. 6c depicts the case $m_1 = 20$ and $CV = 1.2$. It should be remarked that the dependence of the pdf on $\bar{\tau}$ is much greater in the case of $CV = 1.2$ (Fig. 6c) than in $CV = 0.8$ (Fig. 6a) and $CV = 0.5$ (Fig. 6b), which pinpoints the critical role played by CV in this respect. Furthermore, we remark that the shapes of pdf's for different values of $\bar{\tau}$ in the case of $CV = 0.8$ look alike.

3.4 Comparison of the estimates of input parameters between the Wiener model and the OU model

In this section, we compare the estimated input parameters ($\hat{\mu}_0, \hat{\sigma}_0$) for the OU model with those ($\hat{\mu}_w, \hat{\sigma}_w$) for

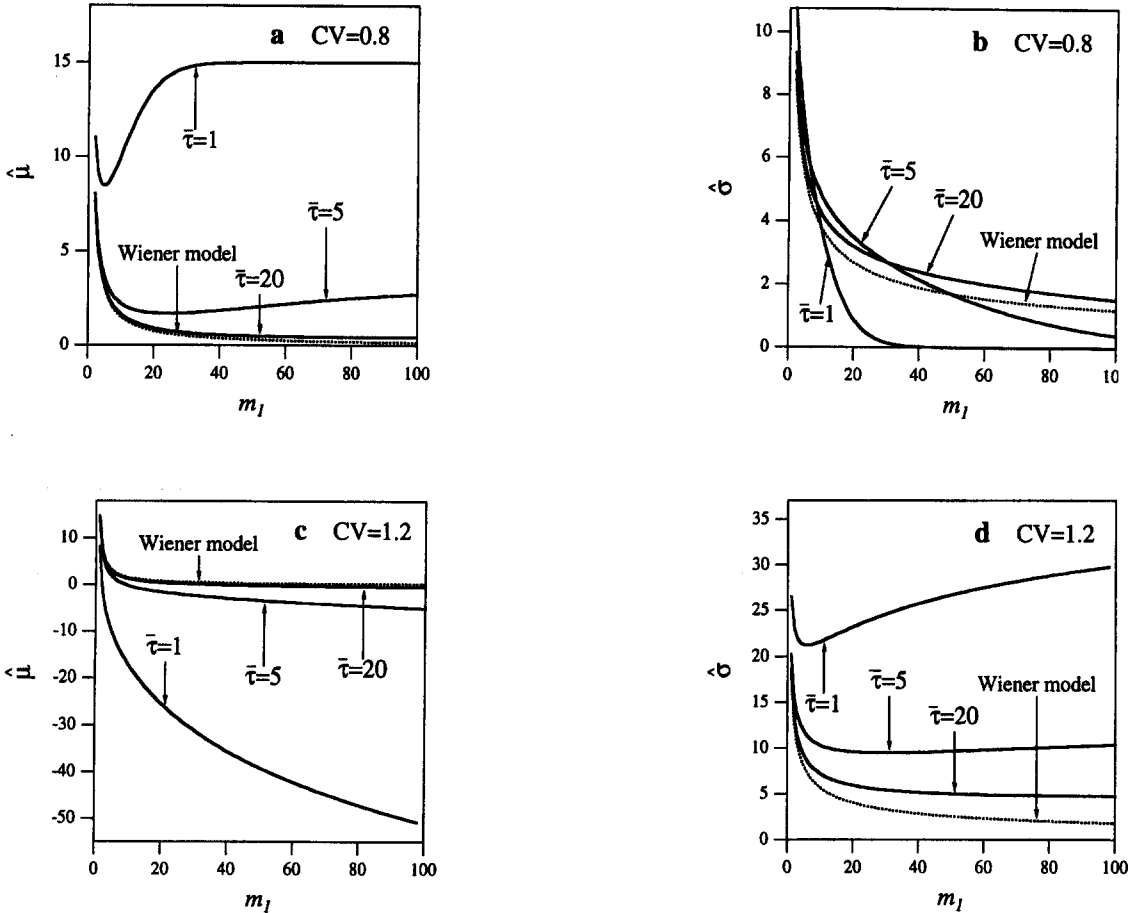


Fig. 7a–d. Comparison of the estimates of input parameters as functions of m_1 , between the Wiener model (dotted line) and the OU model (solid lines) for the following values of the time constant: $\bar{\tau} = 1, 5, 20$.

(a) Values of $\hat{\mu}$ versus m_1 for $CV = 0.8$; (b) values of $\hat{\sigma}$ versus m_1 for $CV = 0.8$; (c) values of $\hat{\mu}$ versus m_1 for $CV = 1.2$; (d) values of $\hat{\sigma}$ versus m_1 for $CV = 1.2$.

the Wiener model. Figure 7a and c show the values of $\hat{\mu}_w$ and $\hat{\mu}_0$ for $\bar{\tau} = 1, 5, 20$ as functions of m_1 for fixed values of CV . Similarly, the values of $\hat{\sigma}_w$ and $\hat{\sigma}_0$ have been plotted in Fig. 7b and d. In agreement with a straightforward theoretical argument, for very small values of m_1 , the estimated parameters for both models are similar, and the range of similarity widens up with $\bar{\tau}$. As m_1 grows larger, the difference in behavior of $\hat{\mu}_w$ and $\hat{\mu}_0$ depends on the values of CV , as for instance shown for $\bar{\tau} = 1, 5$ in Fig. 7a ($CV = 0.8$) and in Fig. 7c ($CV = 1.2$). Moreover, when $CV \geq 1$, $\hat{\mu}_0$ for $\bar{\tau} = 1, 5$ is negative unless m_1 is very small, whereas $\hat{\mu}_w$ is always positive, whatever m_1 . A remarkable different behavior of $\hat{\sigma}_w$ and $\hat{\sigma}_0$ is instead observed in the case $CV = 1.2$ for $\bar{\tau} = 1, 5$ (see Fig. 7d). On the contrary, it is apparent that the estimated parameters for both models behave similarly for $\bar{\tau} = 20$ over a wide and physiologically significant range of m_1 , even though their differences increase with m_1 .

In conclusion, the role of time constant $\bar{\tau}$ is to enhance similarities between the OU and Wiener models for large $\bar{\tau}$ and discrepancies for small $\bar{\tau}$. Hence, if the ratio $M_1 = m_1/\bar{\tau}$ is small, the OU and Wiener models yield similar input parameters. On the other hand, if M_1

is large, one is led to relevantly different estimates of the neuronal input parameters $\hat{\mu}$ and $\hat{\sigma}^2$.

4 Analysis of experimental data

Spontaneous activities of several neurons in the mesencephalic reticular formation (MRF) of head-restricted cats have been recorded in order to investigate their dynamic properties during sleep and wake: during slow-wave sleep (SWS), paradoxical sleep (PS), and the attentive state of bird watching (BIR) (Yamamoto et al. 1986). In this experiment, one could extract activities of a single neuron even though recording was done extracellularly. A set of data consists of 5000 ~ 50 000 ISIs depending on the neurons and their states of consciousness. All ISI histograms constructed from these data exhibit unimodal shapes. We have compared the OU and Wiener neuronal models by determining if the changes of the values of the estimated input parameters are indicative of the varying level of consciousness of the cat. Such a goal has been achieved without any need to proceed to a detailed quantitative comparison of the estimated values of parameters.

Table 2. Statistics of the interspike intervals (ISIs) for mesencephalic reticular formation (MRF) neurons under different states of consciousness and the input parameters estimated via the OU model and the Wiener model. By *PS*, *SWS* and *BIR* we have denoted the states of consciousness during paradoxical sleep, slow-wave sleep, and the attentive state of bird watching respectively

Group	Neuron	State	m_1	CV	$\hat{\mu}_0$	$\hat{\mu}_w$	$\hat{\sigma}_0$	$\hat{\sigma}_w$
I	m113	PS	15.9	0.73	2.09	0.94	3.24	2.76
		SWS	65.9	0.73	2.67	0.23	0.53	1.36
		BIR	22.3	0.66	2.32	0.67	1.95	2.11
	m175	PS	20.2	0.69	2.23	0.74	2.32	2.29
		SWS	49.4	0.57	2.90	0.30	0.20	1.21
		BIR	127	0.66	3.00	0.12	0.00	0.88
II	m171	PS	31.8	1.33	-4.57	0.47	12.5	3.53
		SWS	37.2	1.41	-6.77	0.40	15.0	3.48
		BIR	19.6	1.39	-4.15	0.77	13.7	4.71
	m178	PS	28.4	1.07	-0.70	0.53	6.96	3.02
		SWS	51.9	1.19	-3.29	0.29	9.38	2.47
		BIR	35.8	1.13	-1.74	0.42	8.01	2.84

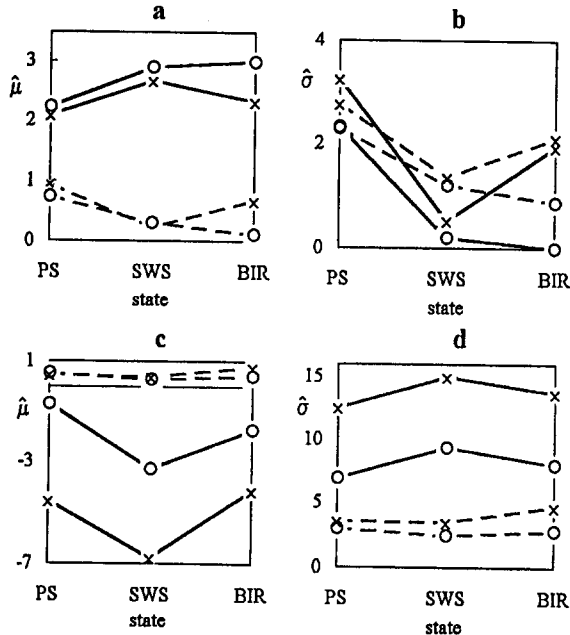


Fig. 8a-d. Estimated values of the input parameters for each MRF neuron at each level of consciousness. *Solid* and *dashed lines* correspond to the estimates for the OU and Wiener model, respectively. **(a)** Values of $\hat{\mu}_w$ and $\hat{\mu}_0$ for each unit in group I. The *cross* corresponds to m113 neuron and the *circle* to m175 neuron. **(b)** Values of $\hat{\sigma}_w$ and $\hat{\sigma}_0$ for group I neurons. **(c)** Values of $\hat{\mu}_w$ and $\hat{\mu}_0$ for each unit in group II. The *cross* corresponds to m171 neuron and the *circle* to m178 neuron. **(d)** Values of $\hat{\sigma}_w$ and $\hat{\sigma}_0$ for group II neurons

Indeed, one of the aims to analyze the firing activities of a neuron in the central nervous system by means of mathematical models is to monitor any significant changes that might occur temporally of its input process as a consequence of the change of the perception level, the presence of long duration constant stimuli, etc.

In Table 2, the mean ISIs and their coefficients of variation are shown for four MRF neurons (neurons m113, m175, m171, and m178). The input parameters ($\hat{\mu}_0$,

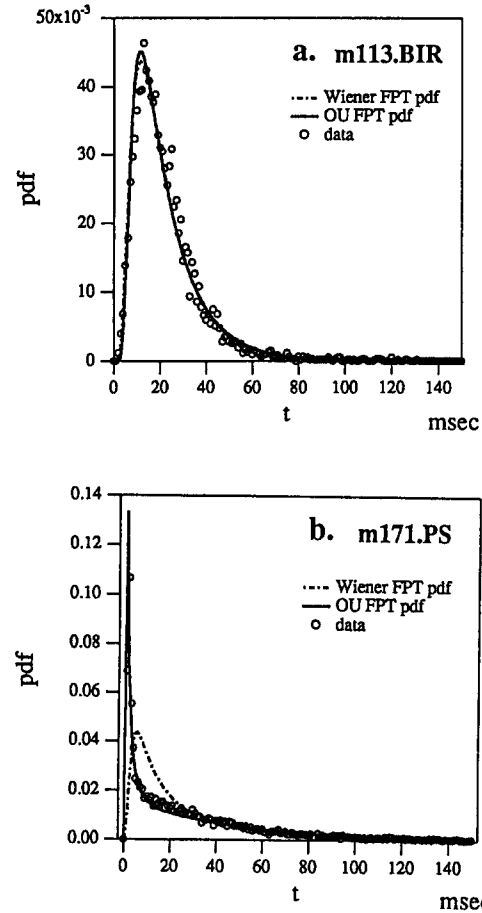


Fig. 9a,b. ISI histograms from the MRF neurons in cat (*circles*) fitted with the OU-FPT pdf's (*solid line*) and the Wiener-FPT pdf's (IG densitis, *dashed line*). **(a)** m113 neuron during BIR; **(b)** m171 neuron during PS

$\hat{\sigma}_0$) and ($\hat{\mu}_w$, $\hat{\sigma}_w$) estimated via the OU model and the Wiener model, respectively, are also reported. We have set $\bar{x}_0 = 0$ mV, $\bar{S} = 15$ mV, and $\bar{\tau} = 5$ ms. We have assumed that the firing process also during PS is a renewal

Table 3. Estimated values of $\hat{\mu}\bar{\sigma}$ as a function of the normalized OU-FPT statistics M_1 and CV. Here we have set $\bar{x}_0 = 0, \bar{\sigma} = 15$

$M_1 \setminus CV$	0.10	0.20	0.30	0.40	0.50	0.60	0.70	0.80	0.90	1.00	1.10	1.20	1.30	1.40	1.50	1.60	1.70	1.80	1.90	2.00
0.50	38.05	37.83	37.45	36.90	36.17	35.25	34.11	32.74	31.13	29.24	27.07	24.58	21.75	18.57	15.00	11.03	6.62	1.76	-3.58	-9.43
1.00	23.66	23.45	23.07	22.51	21.75	20.76	19.50	17.95	16.08	13.85	11.23	8.19	4.70	0.70	-3.80	-8.91	-14.61	-20.94	-27.95	-35.67
1.50	19.24	19.04	18.68	18.13	17.34	16.29	14.92	13.22	11.12	8.50	5.59	2.00	-2.00	-6.69	-12.02	-18.04	-24.79	-32.32	-40.67	-49.83
2.00	17.29	17.11	16.77	16.22	15.42	14.32	12.86	11.01	8.72	5.90	2.55	-1.40	-6.00	-11.29	-17.33	-24.16	-31.83	-40.38	-49.87	-60.32
2.50	16.29	16.13	15.81	15.29	14.48	13.35	11.81	9.82	7.32	4.25	0.57	-3.78	-8.86	-14.71	-21.38	-28.93	-37.40	-46.85	-57.32	-68.85
3.00	15.75	15.61	15.32	14.82	14.02	12.86	11.26	9.14	6.45	3.13	-0.86	-5.59	-11.11	-17.47	-24.72	-32.92	-42.12	-52.36	-63.69	-76.17
3.50	15.44	15.32	15.06	14.59	13.82	12.65	10.99	8.75	5.88	2.32	-0.98	-7.06	-12.99	-19.83	-27.61	-36.40	-46.25	-57.21	-69.32	-82.63
4.00	15.25	15.16	14.94	14.51	13.77	12.60	10.89	8.54	5.49	1.70	-2.88	-8.31	-14.63	-21.90	-30.18	-39.52	-49.96	-61.57	-74.38	-88.45
4.50	15.15	15.07	14.88	14.50	13.80	12.65	10.90	8.45	5.23	1.21	-3.65	-9.40	-16.09	-23.78	-32.51	-42.35	-53.34	-65.54	-79.00	-93.75
5.00	15.05	15.02	14.87	14.53	13.88	12.76	10.99	8.44	5.06	0.82	-4.32	-10.38	-17.42	-25.49	-34.65	-44.96	-56.46	-69.21	-83.25	-98.63
5.50	15.05	15.00	14.87	14.58	13.99	12.91	11.13	8.50	4.95	0.49	-4.91	-11.27	-18.64	-27.08	-36.64	-47.38	-59.36	-72.61	-87.20	-103.16
6.00	15.03	14.99	14.89	14.64	14.10	13.08	11.31	8.59	4.89	0.21	-5.44	-12.09	-19.78	-28.57	-38.50	-49.65	-62.07	-75.79	-90.88	-107.35
6.50	15.02	14.99	14.95	14.69	14.22	13.25	11.50	8.73	4.87	-0.03	-6.38	-13.57	-21.85	-31.28	-41.91	-53.81	-67.02	-81.61	-97.61	-115.08
7.00	15.01	14.99	14.92	14.74	14.33	13.43	11.71	8.88	4.87	-0.23	-6.80	-14.25	-22.81	-32.54	-43.49	-55.73	-69.31	-84.28	-100.70	-118.61
7.50	15.01	14.99	14.94	14.79	14.43	13.60	11.93	9.06	4.90	-0.41	-7.19	-14.89	-24.59	-34.87	-46.42	-59.29	-73.55	-89.25	-106.43	-125.15
8.00	15.00	14.99	14.96	14.86	14.60	13.91	12.37	9.45	5.02	-0.71	-7.56	-15.51	-25.42	-35.97	-47.79	-60.96	-75.53	-91.56	-109.10	-128.19
8.50	15.00	14.99	14.97	14.89	14.66	14.05	12.58	9.66	5.09	-0.84	-7.91	-16.09	-25.42	-35.97	-47.79	-60.96	-75.53	-91.56	-109.10	-128.19
9.00	15.00	14.99	14.98	14.91	14.72	14.18	12.78	9.87	5.18	-0.95	-8.25	-16.66	-26.23	-37.02	-49.11	-62.56	-77.43	-93.78	-111.65	-131.10
9.50	15.00	15.00	14.98	14.92	14.77	14.29	12.98	10.09	5.28	-1.05	-8.57	-17.20	-27.00	-38.04	-50.38	-64.10	-79.25	-95.90	-114.10	-133.88
10.00	15.00	15.00	14.98	14.93	14.77	14.29	12.98	10.09	5.28	-1.05	-8.57	-17.20	-27.00	-38.04	-50.38	-64.10	-79.25	-95.90	-114.10	-133.88
12.00	15.00	15.00	14.99	14.98	14.90	14.62	13.65	10.96	5.73	-1.38	-9.73	-19.20	-29.84	-41.76	-55.02	-69.72	-85.90	-103.64	-122.98	-143.98
14.00	15.00	15.00	14.98	14.94	14.96	14.80	14.14	11.78	6.26	-1.63	-10.76	-20.98	-32.37	-45.05	-59.11	-74.65	-91.72	-110.39	-130.71	-152.74
16.00	15.00	15.00	15.00	14.98	14.98	14.90	14.47	12.50	6.83	-1.81	-11.69	-22.59	-34.65	-48.01	-62.78	-79.05	-96.89	-116.38	-137.56	-160.49
18.00	15.00	15.00	15.00	15.00	14.99	14.95	14.68	13.11	7.43	-1.96	-12.54	-24.07	-36.73	-50.69	-66.09	-83.02	-101.55	-121.76	-143.71	-167.43
20.00	15.00	15.00	15.00	15.00	15.00	14.98	14.81	13.60	8.04	-2.08	-13.34	-25.43	-38.64	-53.16	-69.12	-86.64	-105.80	-126.66	-149.28	-173.72
22.00	15.00	15.00	15.00	15.00	15.00	14.99	14.89	13.98	8.64	-2.18	-14.08	-26.71	-40.42	-55.44	-71.92	-89.97	-109.69	-131.14	-154.38	-194.48
24.00	15.00	15.00	15.00	15.00	15.00	14.99	14.94	14.27	9.24	-2.26	-14.78	-27.91	-42.08	-57.56	-74.51	-93.06	-113.29	-135.28	-159.09	-184.77
26.00	15.00	15.00	15.00	15.00	15.00	15.00	14.96	14.48	9.82	-2.33	-15.44	-29.03	-43.63	-59.54	-76.93	-95.93	-116.63	-139.12	-163.45	-189.68
28.00	15.00	15.00	15.00	15.00	15.00	15.00	14.98	14.63	10.37	-2.40	-16.07	-30.10	-45.09	-61.39	-79.19	-98.61	-119.76	-142.70	-167.52	-194.25
30.00	15.00	15.00	15.00	15.00	15.00	15.00	14.99	14.74	10.90	-2.45	-16.67	-31.10	-46.67	-63.14	-81.32	-101.13	-122.69	-146.06	-171.33	-198.53
32.00	15.00	15.00	15.00	15.00	15.00	15.00	14.99	14.82	11.39	-2.50	-17.25	-32.06	-47.78	-64.88	-83.33	-103.51	-125.45	-149.23	-174.91	-202.55
34.00	15.00	15.00	15.00	15.00	15.00	15.00	15.00	14.88	11.84	-2.54	-17.80	-32.98	-49.03	-66.37	-85.23	-105.76	-128.06	-152.21	-178.29	-206.35
36.00	15.00	15.00	15.00	15.00	15.00	15.00	15.00	14.91	12.25	-2.58	-18.34	-33.86	-50.22	-67.86	-87.04	-107.89	-130.53	-155.04	-181.49	-209.94
38.00	15.00	15.00	15.00	15.00	15.00	15.00	15.00	14.94	12.63	-2.61	-18.85	-34.70	-51.35	-69.29	-88.76	-109.92	-132.88	-157.73	-184.53	-213.34
40.00	15.00	15.00	15.00	15.00	15.00	15.00	15.00	14.96	12.96	-2.64	-19.34	-35.50	-52.43	-70.65	-90.40	-111.86	-135.12	-160.29	-187.42	-216.58
42.00	15.00	15.00	15.00	15.00	15.00	15.00	15.00	14.97	13.25	-2.67	-19.82	-36.27	-53.47	-71.95	-91.97	-113.70	-137.26	-162.73	-190.18	-219.67
44.00	15.00	15.00	15.00	15.00	15.00	15.00	15.00	14.98	13.51	-2.70	-20.28	-37.02	-54.47	-73.20	-93.48	-115.47	-139.31	-165.06	-192.82	-222.63
46.00	15.00	15.00	15.00	15.00	15.00	15.00	15.00	14.99	13.74	-2.72	-20.73	-37.74	-55.43	-74.40	-94.92	-117.17	-141.27	-167.30	-195.34	-225.46
48.00	15.00	15.00	15.00	15.00	15.00	15.00	15.00	14.99	13.93	-2.74	-21.17	-38.43	-56.36	-75.55	-96.31	-118.80	-143.15	-169.45	-197.77	-228.17
50.00	15.00	15.00	15.00	15.00	15.00	15.00	15.00	14.99	14.10	-2.76	-21.59	-39.10	-57.25	-76.67	-97.65	-120.37	-144.96	-171.51	-200.10	-230.77

Table 4. Estimated values of $\hat{\sigma}\sqrt{\bar{\tau}}$ as a function of M_1 and CV for the same choice \bar{x}_0 and \bar{S} as in Table 3

M_1	CV																			
	0.10	0.20	0.30	0.40	0.50	0.60	0.70	0.80	0.90	1.00	1.10	1.20	1.30	1.40	1.50	1.60	1.70	1.80	1.90	2.00
0.50	2.06	4.16	6.32	8.58	10.95	13.46	16.12	18.96	21.98	25.20	28.64	32.30	36.21	40.37	44.80	49.50	54.50	59.81	65.43	71.37
1.00	1.34	2.73	4.23	5.87	7.67	9.65	11.84	14.26	16.92	19.83	23.02	26.50	30.29	34.41	38.87	43.68	48.86	54.43	60.40	66.79
1.50	0.95	1.98	3.15	4.49	6.04	7.81	9.82	12.10	14.67	17.54	20.73	24.25	28.14	32.39	37.04	42.10	47.58	53.50	59.88	66.72
2.00	0.69	1.47	2.42	3.56	4.94	6.58	8.51	10.74	13.30	16.20	19.45	23.08	27.10	31.53	36.40	41.70	47.47	53.72	60.47	67.71
2.50	0.50	1.10	1.87	2.86	4.11	5.66	7.54	9.76	12.34	15.29	18.63	22.38	26.55	31.16	36.23	41.78	47.82	54.36	61.42	69.02
3.00	0.35	0.81	1.44	2.30	3.44	4.92	6.76	8.98	11.60	14.62	18.06	21.94	26.26	31.05	36.31	42.08	48.35	55.16	62.51	70.41
3.50	0.25	0.60	1.10	1.84	2.88	4.29	6.10	8.33	11.00	14.10	17.65	21.65	26.12	31.07	36.52	42.48	48.98	56.02	63.62	71.79
4.00	0.18	0.43	0.84	1.47	2.41	3.74	5.52	7.77	10.50	13.69	17.34	21.47	26.07	31.18	36.80	42.94	49.64	56.89	64.72	73.13
4.50	0.12	0.31	0.64	1.17	2.01	3.27	5.01	7.28	10.06	13.34	17.10	21.35	26.09	31.34	37.12	43.43	50.30	57.75	65.78	74.41
5.00	0.08	0.23	0.48	0.93	1.67	2.85	4.56	6.84	9.68	13.05	16.92	21.28	26.15	31.54	37.46	43.93	50.97	58.59	66.81	75.63
5.50	0.06	0.16	0.36	0.73	1.39	2.48	4.14	6.44	9.34	12.79	16.77	21.25	26.24	31.75	37.81	44.43	51.62	59.40	67.79	76.79
6.00	0.04	0.11	0.27	0.57	1.14	2.15	3.76	6.06	9.03	12.57	16.65	21.24	26.34	31.98	38.17	44.92	52.25	60.18	68.72	77.89
6.50	0.03	0.08	0.20	0.44	0.94	1.85	3.41	5.72	8.74	12.38	16.56	21.25	26.47	32.22	38.53	45.40	52.87	60.93	69.62	78.94
7.00	0.02	0.06	0.15	0.34	0.77	1.60	3.09	5.39	8.47	12.20	16.48	21.28	26.60	32.46	38.88	45.87	53.46	61.66	70.48	79.93
7.50	0.01	0.04	0.11	0.27	0.62	1.37	2.79	5.08	8.23	12.04	16.42	21.32	26.74	32.71	39.23	46.33	54.04	62.35	71.30	80.88
8.00	0.01	0.03	0.08	0.21	0.50	1.17	2.51	4.79	7.99	11.90	16.37	21.37	26.89	32.95	39.57	46.78	54.59	63.02	72.08	81.79
8.50	0.01	0.02	0.06	0.16	0.41	1.00	2.26	4.52	7.77	11.77	16.34	21.43	27.04	33.19	39.91	47.22	55.13	63.66	72.83	82.65
9.00	0.00	0.01	0.04	0.12	0.33	0.85	2.03	4.26	7.56	11.65	16.31	21.49	27.19	33.43	40.24	47.64	55.64	64.28	73.55	83.48
9.50	0.00	0.01	0.03	0.09	0.26	0.72	1.82	4.01	7.36	11.54	16.29	21.56	27.34	33.67	40.56	48.05	56.14	64.87	74.24	84.27
10.00	0.00	0.01	0.02	0.07	0.21	0.61	1.63	3.77	7.17	11.43	16.28	21.63	27.49	33.90	40.88	48.44	56.63	65.44	74.91	85.03
12.00	0.00	0.00	0.01	0.02	0.09	0.31	1.02	2.92	6.46	11.08	16.27	21.94	28.10	34.79	42.06	49.92	58.41	67.54	77.33	87.80
14.00	0.00	0.00	0.00	0.01	0.03	0.15	0.62	2.22	5.84	10.81	16.32	22.26	28.68	35.62	43.13	51.25	59.99	69.39	79.45	90.19
16.00	0.00	0.00	0.00	0.00	0.01	0.07	0.37	1.66	5.27	10.58	16.40	22.59	29.23	36.38	44.11	52.44	61.40	71.02	81.32	92.30
18.00	0.00	0.00	0.00	0.00	0.01	0.03	0.21	1.22	4.75	10.39	16.49	22.91	29.75	37.09	45.00	53.52	62.67	72.49	82.99	94.19
20.00	0.00	0.00	0.00	0.00	0.00	0.02	0.12	0.88	4.27	10.22	16.60	23.22	30.23	37.75	45.82	54.50	63.83	73.82	84.50	95.88
22.00	0.00	0.00	0.00	0.00	0.00	0.01	0.07	0.63	3.82	10.08	16.72	23.52	30.70	38.36	46.58	55.41	64.89	75.04	85.88	97.42
24.00	0.00	0.00	0.00	0.00	0.00	0.00	0.04	0.44	3.40	9.96	16.84	23.81	31.13	38.93	47.28	56.25	65.86	76.15	87.14	98.84
26.00	0.00	0.00	0.00	0.00	0.00	0.00	0.02	0.31	3.01	9.84	16.96	24.09	31.54	39.46	47.94	57.03	66.77	77.18	88.30	100.14
28.00	0.00	0.00	0.00	0.00	0.00	0.00	0.01	0.21	2.65	9.74	17.08	24.36	31.93	39.96	48.55	57.75	67.61	78.14	89.38	101.34
30.00	0.00	0.00	0.00	0.00	0.00	0.00	0.01	0.15	2.31	9.65	17.20	24.62	32.30	40.44	49.13	58.43	68.39	79.04	90.39	102.46
32.00	0.00	0.00	0.00	0.00	0.00	0.00	0.10	2.01	9.57	17.32	24.86	32.65	40.88	49.67	59.07	69.13	79.88	91.33	103.51	
34.00	0.00	0.00	0.00	0.00	0.00	0.00	0.07	1.74	9.49	17.44	25.10	32.98	41.31	50.18	59.68	69.83	80.67	92.22	104.50	
36.00	0.00	0.00	0.00	0.00	0.00	0.00	0.05	1.50	9.42	17.56	25.33	33.30	41.71	50.67	60.25	70.48	81.41	93.05	105.43	
38.00	0.00	0.00	0.00	0.00	0.00	0.00	0.03	1.28	9.35	17.67	25.55	33.60	42.09	51.13	60.79	71.10	82.11	93.84	106.30	
40.00	0.00	0.00	0.00	0.00	0.00	0.00	0.02	1.09	9.29	17.79	25.76	33.90	42.46	51.57	61.30	71.69	82.78	94.59	107.13	
42.00	0.00	0.00	0.00	0.00	0.00	0.00	0.02	0.93	9.23	17.90	25.96	34.17	42.81	51.99	61.79	72.25	83.41	95.30	107.92	
44.00	0.00	0.00	0.00	0.00	0.00	0.00	0.01	0.78	9.17	18.01	26.16	34.44	43.14	52.39	62.25	72.79	84.02	95.97	108.67	
46.00	0.00	0.00	0.00	0.00	0.00	0.00	0.01	0.66	9.12	18.12	26.35	34.70	43.46	52.77	62.70	73.30	84.59	96.62	109.39	
48.00	0.00	0.00	0.00	0.00	0.00	0.00	0.00	0.55	9.08	18.22	26.53	34.95	43.77	53.14	63.13	73.79	85.15	97.23	110.07	
50.00	0.00	0.00	0.00	0.00	0.00	0.00	0.00	0.46	9.03	18.32	26.71	35.19	44.07	53.49	63.54	74.25	85.67	97.82	110.72	

process (however, see Yamamoto et al. 1986), because our aim in this section is to give an example of the application of our estimation method and also to compare the input parameters as estimated via the two alternative diffusion models (Wiener and OU). The high reliability of the available data as well as the existence of numerous ISIs of very short duration have led us to ignore refractoriness, as far as the present analysis is concerned. Analysis of the spontaneous activities of MRF neurons will be the object of future investigations.

Let us focus our attention on the CV of the ISI. One may classify the four neurons into two groups, depending on whether CV is greater or less than unity. One group (denoted as group I) consists of neurons m113 and m175, in which $CV < 1$ for all three levels of consciousness. The other (group II) consists of neurons m171 and m178, in which $CV > 1$ for all three levels of consciousness. Figure 8 depicts the dependence of the estimated values of parameters on the levels of consciousness for each group. Figure 8a and b refer to group I and Fig. 8c and d to group II. For neurons in group I, though both models yield positive estimates of the mean input μ , the values of $\hat{\mu}_0$ are much larger than those of $\hat{\mu}_w$, and $\hat{\mu}_0$ attains its minimum at the PS stage, whereas $\hat{\mu}_w$ reaches its

maximum in the PS state for both neurons (Fig. 8a). The changes of the estimates of σ for both models are instead similar to each other for both neurons in this group, and their sizes are rather close to each other for each stage (Fig. 8b). For neurons of group II, the estimated values $\hat{\mu}_w$ are positive and orders of magnitudes are almost the same as those for neurons of group I (see Fig. 8a, c and Table 2). On the contrary, the values of $\hat{\mu}_0$ are negative. The values of $\hat{\sigma}_0$ are much larger than those of $\hat{\sigma}_w$ (Fig. 8d). Moreover, their behaviors when passing through the different sleep conditions are fundamentally different for the Wiener and the OU model.

By using $\bar{\tau}$ and the estimated parameters $\hat{\xi}$ and $\hat{\eta}$ which are obtained in the estimation procedure (see Sect. 3.1), we can also determine the estimated OU-FPT pdf. The ISI histogram can, then, be fitted by the OU-FPT pdf. The ISI histograms for neurons of group I are fitted well by both OU-FPT pdf and by the IGD (i.e. the FPT pdf for Wiener model), irrespective of the sleep stages (see Fig. 9a). On the contrary, the fitting of the IGD to the ISI histograms for neurons of group II is not as good as in the former case (see Fig. 9b). Such results are in full agreement with the conclusions earlier drawn on the theoretical comparison of the two models (see also Fig. 6).

5 Discussion

A quantitative analysis of spontaneous activities of single neurons by means of the OU model in terms of the first two moments of the ISIs has been proposed. The estimated input parameters for this model can be obtained either by encoding the above estimating procedure on a computer or, more directly, by making use of Tables 3 and 4 for the estimated input parameters. Our tables permit us to estimate the input parameters from the sample ISI for the OU model no matter what values of neuronal parameters are chosen. In such a sense, we may say that Tables 3 and 4 provide the basic tool for neuronal parameters-fitting tasks.

We have checked the relation between the estimated input parameters and the ISI statistics in the OU model. The following conclusions clearly emerged

1. when the coefficient of variation is less than unity ($CV \leq 1$), an increase of the mean firing time does not necessarily imply a decrease of the input mean $\hat{\mu}$. A small amount of input noise considerably accelerates the firing.
2. the value of the CV of the ISI plays a crucial role in this estimation, and hence it would be a better indicator of input parameters than the firing rate. Condition $CV < 1$ ($CV \geq 1$) roughly implies that $\hat{\mu}$, the mean input per unit time, is positive (negative). For more details, see text and also Tuckwell (1979), Wilbur and Rinzel (1983), and Musila and Lánský (1991). The CV also reflects the degree of irregularity in the input process.

The estimated parameters for the OU models with different time constants and for the Wiener model have been compared. The value of the time constant τ affects considerably the resulting estimated values of parameters. It should be mentioned explicitly that in principle it is possible to estimate input parameters μ and σ as well as the time constant τ by means of the first, second, and third-order FPT moments for fixed values of x_0 and S . This procedure has been explored by us and successfully implemented. However, the parameters thus estimated appear to be rather unreliable, being too much influenced by small fluctuations of the FPT moments.

Comparison of estimated parameters for the two diffusion models suggests that the Wiener model is not suitable to mimic firing activities in which the firing rate is rather low compared with the time constant (i.e. when M_1 is not small), even if the fitness of IGD to the ISI histogram is good. On the other hand, it appears that for the estimation of input parameters the Wiener model can be used in place of the OU model for neurons whose membrane time constant is relatively large or for neurons characterized by massive excitatory inputs and exhibiting high frequency firing activity.

This estimation method has been applied to experimental data of single neurons' spontaneous activities in the MRF of head-restricted cats during sleep and wake: during slow-wave sleep, paradoxical sleep, and the attentive state of bird watching (Yamamoto et al. 1986). The time constant of the OU model was set to 5 ms, as

indicated in the literature for mammalian neurons (cf. Wilbur and Rinzel 1983). Behaviors of estimated input parameters when passing through the different sleep conditions have been seen to be quite different for the Wiener and OU models.

Acknowledgements. We are indebted to Professor M. Yamamoto of Tohoku University for providing us the data of spontaneous activities of MRF neurons. We also express our gratitude to anonymous referees for some helpful comments. This work was partly supported by Grants-in-Aid for Scientific Research on Priority Areas (1) Nos. 02255105, 03251105, 04246104 and (2)05267232, Monbusho International Scientific Research Program: Joint Research No. 05044099, the Japanese Ministry of Education, Science and Culture. One of us (L.M.R.) acknowledges support from the Italian CNR and MURST (40% funds).

List of symbols

- $X(t)$: The Ornstein-Uhlenbeck (OU) process
 T_S : The first-passage time (FPT) to a constant boundary S for the OU process $X(t)$ starting at x_0
 μ : The constant drift of the OU process or the mean input per unit time to a neuron for the OU model
 $\hat{\mu}, \hat{\mu}_0$: The estimate of μ
 $\hat{\mu}_w$: The estimated constant drift of the Wiener process or the mean input per unit time to a neuron for the Wiener model
 σ : The infinitesimal standard deviation of the OU process or the input standard deviation per unit time to a neuron for the OU model
 $\hat{\sigma}, \hat{\sigma}_0$: The estimate of σ
 $\hat{\sigma}_w$: The estimated infinitesimal standard deviation of the Wiener process or input standard deviation per unit time for the Wiener model
 x_0 : The initial value of the OU process or the difference of the initial membrane potential from the resting potential
 S : The difference between the resting potential and the threshold potential
 τ : The membrane time constant of a neuron
 \bar{x}_0, \bar{S} , and $\bar{\tau}$: A preassigned value for x_0, S , and τ , respectively
 $X'(t')$: The 'normalized' OU process
 ξ : The initial value of the 'normalized' OU process
 η : The threshold value in the 'normalized' OU process
 $\hat{\xi}$ and $\hat{\eta}$: The estimate of ξ and η , respectively
 $g(t|S, x_0)$: The FPT probability density function (pdf) of the OU process $X(t)$
 $g'(t'|\eta, \xi)$: The FPT pdf of the normalized OU process $X'(t')$
 m_1 : The first moment about the origin of the FPT for the OU process $X(t)$ or the sample mean of the interspike intervals (ISIs)
 m_2 : The second moment about the origin of the FPT for the OU process $X(t)$ or the second sample moment of the ISIs
 M_1 : The first moment about the origin of the FPT for the normalized OU process or the sample mean of the ISIs normalized by $\bar{\tau}$ ($M_1 \equiv m_1/\bar{\tau}$)
 CV : The coefficient of variation of the FPT of the OU process $X(t)$ and of the normalized OU process $X'(t')$ or the sample coefficient of variation of the ISIs and of the

ISIs normalized by $\bar{\tau}$ (CV \equiv standard deviation/mean) PS, SWS, and BIR: paradoxical sleep, slow-wave sleep, and the attentive state of bird watching

Appendix Tables of estimates

Tables 3 and 4 list values of $\hat{\mu}\bar{\tau}$ and $\hat{\sigma}\sqrt{\bar{\tau}}$ as functions of the FPT mean M_1 of the normalized OU process and of the CV, having fixed \bar{x}_0 and S to the values 0 and 15, respectively. M_1 has been made to change in the range of 0.5 ~ 50 and CV in the range of 0.1 ~ 2, both neurophysiologically meaningful. In those cases where values of $\bar{x}_0 = 0$ and $S = 15$ are not appropriate for the neuron used in the experiment, the estimates $\hat{\mu}_N\bar{\tau}$ and $\hat{\sigma}_N\sqrt{\bar{\tau}}$ can be easily obtained from (15) as follows

$$\hat{\mu}_N = \frac{\xi S_N - \hat{\eta}\bar{x}_{0N}}{15\xi} \hat{\mu}_t, \quad \hat{\sigma}_N = \frac{S_N - \bar{x}_{0N}}{15} \hat{\sigma}_t \quad (19)$$

where S_N and \bar{x}_{0N} denote the new assumed values of the threshold and of equilibrium state and where $\hat{\mu}_t$ and $\hat{\sigma}_t$ denotes the estimated values obtained from Tables 3 and 4. The values of ξ and $\hat{\eta}$ are obtained as

$$\xi = \sqrt{\frac{2}{\hat{\sigma}_t^2 \bar{\tau}}} \hat{\mu}_t \bar{\tau}, \quad \hat{\eta} = \sqrt{\frac{2}{\hat{\sigma}_t^2 \bar{\tau}}} \hat{\mu}_t (15 - \bar{\tau})$$

To illustrate our method for determining input parameters in the case of arbitrary initial state and threshold, let us give an example. Suppose we are given a set of data that we assume to be generated by a neuron characterized by intrinsic parameters $\bar{x}_0 = 0$ mV, $S = 10$ mV, and $\bar{\tau} = 5$ ms. Let the sample mean m_1 of the ISI be 30 ms and its CV = 0.8. Then the sample mean M_1 normalized by $\bar{\tau}$ equals 6. For the case $\bar{x}_0 = 0$ and $S = 15$, the quantities $\hat{\mu}\bar{\tau}$ and $\hat{\sigma}\sqrt{\bar{\tau}}$ are obtained from Tables 3 and 4, respectively. We find $5\hat{\mu}_t = 8.59$ and $\sqrt{5}\hat{\sigma}_t = 6.06$, respectively. As a consequence, $\hat{\mu}_t = 1.72$ and $\hat{\sigma}_t = 2.71$. These values correspond to the choices $\bar{x}_0 = 0$ and $S = 15$. From (19), we finally obtain $\hat{\mu}_N = 1.15$ (mV/ms) and $\hat{\sigma}_N = 1.81$ (mV/ $\sqrt{\text{ms}}$) for the considered case $S = 10$ and $\bar{x}_0 = 0$.

References

- Anastasio TJ, Correia MJ, Perachio AA (1985) Spontaneous and driven responses of semicircular canal primary afferents in the unanesthetized pigeon. *J Neurophysiol* 54:335–347
- Buonocore A, Nobile AG, Ricciardi LM (1987) A new integral equation for the evaluation of first-passage-time probability densities. *Adv Appl Prob* 19:784–800
- Capocelli RM, Ricciardi LM (1973) A continuous Markovian model for neuronal activity. *J Theor Biol* 40:369–387
- Correia MJ, Landolt JP (1977) A point process analysis of the spontaneous activity of anterior semicircular canal unit in the anesthetized pigeon. *Biol Cybern* 27:199–213
- Gerstein GL, Mandelbrot B (1964) Random walk models for the spike activity of a single neuron. *Biophys J* 4:41–68
- Giorno V, Lansky P, Nobile AG, Ricciardi LM (1988) Diffusion approximation and first-passage-time problem for a model neuron. III. A birth-and-death process approach. *Biol Cybern* 58:387–404
- Giorno V, Nobile AG, Ricciardi LM (1990) On the asymptotic behaviour of first-passage-time densities for one-dimensional diffusion processes and varying boundaries. *Adv Appl Prob* 22:883–914
- Habib MK (1992) Optimal estimation for semimartingale neuronal models. *J Stat Plan Inference* 33:143–156
- Hanson FB, Tuckwell HC (1983) Diffusion approximation for neuronal activity including synaptic reversal potential. *J Theor Neurobiol* 2:127–153
- Kandel ER, Schwartz JH (1985) Principles of neural science, 2nd edn. Elsevier, New York
- Keilson J, Ross HF (1975) Passage time distributions for gaussian Markov (Ornstein Uhlenbeck) statistical processes. Selected tables in mathematical statistics, Vol III. American Mathematical Society, pp 233–327
- Lánský P (1983) Inference for the diffusion models of neuronal activity. *Math Biosci* 67:247–260
- Lánský P, Lánská V (1987) Diffusion approximation of the neuronal model with synaptic reversal potentials. *Biol Cybern* 56:19–26
- Lánský P, Radil T (1987) Statistical inference on spontaneous neuronal discharge patterns. *Biol Cybern* 55:299–311
- Lánský P, Giorno V, Nobile AG, Ricciardi LM (1988) A diffusion neuronal model and its parameters. In: Ricciardi LM (ed) Biomathematics and related computational problems. Kluwer, Dordrecht, pp 27–37
- Lánský P, Smith CE, Ricciardi LM (1990) One-dimensional stochastic diffusion models of neuronal activity and related first passage time problems. *Trends Biol Cybern* 1:153–162
- Levine MW (1991) The distribution of the intervals between neural impulses in the maintained discharges of retinal ganglion cells. *Biol Cybern* 65:459–467
- Musila M, Lánský P (1991) Generalized Stein's model for anatomically complex neurons. *Biosystems* 25:179–191
- Nobile A, Ricciardi LM, Sacerdote L (1985) Exponential trends of Ornstein-Uhlenbeck first passage time densities. *J Appl Prob* 22:360–369
- Ortega JM, Rheinboldt WC (1970) Iterative solution of nonlinear equations in several variables. Academic Press, New York
- Ricciardi LM (1976) Diffusion approximation for a multi-input model neuron. *Biol Cybern* 24:237–240
- Ricciardi LM (1977) Diffusion processes and related topics in biology. (Lecture notes in Biomathematics, Vol 14) Springer, Berlin Heidelberg New York
- Ricciardi LM, Sato S (1988) First-passage-time density and moments of the Ornstein-Uhlenbeck process. *J Appl Prob* 25:43–57
- Rospars JP, Lánský P (1993) Stochastic model neuron without resetting of dendritic potential: application to the olfactory system. *Biol Cybern* 69:283–294
- Roy K, Smith DR (1969) Analysis of the exponential decay model of the neuron showing frequency threshold effects. *Bull Math Biophys* 31:341–357
- Smith CE, Smith MV (1984) Moments of voltage trajectories for Stein's model with synaptic reversal potentials. *J Theor Neurobiol* 3:67–77
- Tuckwell HC (1979) Synaptic transmission in a model for stochastic neuronal activity. *J Theor Biol* 77:65–81
- Tuckwell HC (1982) Neuronal firing and input variability. *J Theor Neurobiol* 1:197–218
- Tuckwell HC (1988) Introduction to theoretical neurobiology, Vol. 2. Nonlinear and stochastic theories. Cambridge University Press, New York
- Tuckwell HC (1989) Stochastic processes in the neurosciences. CBMS 56, SIAM
- Tuckwell HC, Richter W (1978) Neuronal interspike time distribution and the estimation of neurophysiological and neuroanatomical parameters. *J Theor Biol* 71:167–183
- Wilbur WJ, Rinzel J (1983) A theoretical basis for large coefficient of variation and bimodality in neuronal interspike interval distributions. *J Theor Biol* 105:345–368
- Yamamoto M, Nakahama H, Shima K, Komada T, Mushiake H (1986) Markov-dependency and spectral analyses on spike counts in mesencephalic reticular neurons during sleep and attentive states. *Brain Res* 366:279–289